Ionic liquid-mediated regeneration of cellulose dramatically improves decrystallization, TEMPO-mediated oxidation and alkyl/alkenyl succinylation

International Journal of Biological Macromolecules 236 (2023) 123983

Contents lists available at ScienceDirect

International Journal of Biological Macromolecules

journal homepage: www.elsevier.com/locate/ijbiomac

Ionic liquid-mediated regeneration of cellulose dramatically improves decrystallization, TEMPO-mediated oxidation and alkyl/alkenyl succinylation

Ziqian Li [a], Guoqiang Zhang [b], Dimitris Charalampopoulos [b], Zheng Guo [a,*]

[a] Department of Biological and Chemical Engineering, Gustav weids vej 10A, Faculty of Technical Science, Aarhus University, 8000 Aarhus, Denmark
[b] Department of Food and Nutritional Sciences, University of Reading, Whiteknights, Reading RG6 6AP, United Kingdom

ARTICLE INFO

Keywords:
Ionic liquids
Succinylation
Emulsifier
TEMPO-mediated oxidation
Cellulose
Antioxidation

ABSTRACT

This work demonstrated a successful strategy that simple ionic liquids (ILs) mediated pretreatment could effectively reduce crystallinity of cellulose from 71 % to 46 % (by C_2MIM.Cl) and 53 % (by C_4MIM.Cl). The IL-mediated regeneration of cellulose greatly promoted its reactivity for TEMPO-catalyzed oxidation, which the resulting COO^- density (mmol/g) increased from 2.00 for non-IL-treated cellulose to 3.23 (by C_2MIM.Cl) and 3.42 (C_4MIM.Cl); and degree of oxidation enhanced from 35 % to 59 % and 62 %, respectively. More significantly, the yield of oxidized cellulose increased from 4 % to 45–46 %, by 11-fold. IL-regenerated cellulose can also be directly subjected to alkyl/alkenyl succinylation without TEMPO-mediated oxidation, producing nanoparticles with properties similar to oxidized celluloses (55-74 nm in size, −70–79 mV zeta-potential and 0.23–0.26 PDI); but in a much higher overall yield (87–95 %) than IL-regeneration-coupling-TEMPO-oxidation (34–45 %). Alkyl/alkenyl succinylated TEMPO-oxidized cellulose showed 2–2.5 times higher ABTS* scavenging ability than non-oxidized cellulose; however, alkyl/alkenyl succinylation also resulted in a significant decline in Fe^{2+} chelating property.

1. Introduction

Cellulose is the most abundant naturally occurring biopolymer with an annual production of 1.5×10^{12} tons [1]. Due to its unique renewability, biocompatibility, biodegradability, and chemical modifiability, cellulose as a kind of natural materials having huge industrial application potential, has attracted increasing attention from industry sectors and scientific community. To produce cellulose-based value-added materials, chemical/enzymatic modification and derivation of cellulose are necessary to cartelize their properties for demanded applications. Cellulose is composed of repeated units of anhydroglucose linked by 1–4 glycosidic linkages [2]. Based on the reaction of the free hydroxyl groups in the anhydroglucose units available for functionalization, derivatization processes, such as oxidation, esterification, etherification, and succinylation could endow cellulose with different functionalities for a broad range of applications. Succinylation, which incorporates hydrophobic alkyl/alkenyl succinyl groups into hydrophilic biopolymer, could produce amphiphilic biopolymer-based emulsifiers. Water-soluble polysaccharides including starch [3–7] or protein [8–13] after the succinylation could significantly improve their emulsifying ability thanks to the enhanced amphiphilic balance achieved by alkyl/alkenyl succinylation [14–17]. However, the studies on alkyl/alkenyl succinylation of cellulose were rarely reported. Natural cellulose's inherent insolubility in water and most organic solvent solutions is a major obstacle as to engender such a reaction for cellulose modification is challenging [18]. Cellulose is also a kind of high-crystalline fibril that is assembled by the entanglement of microfibril chains with one another via extensive intra- and inter-chain hydrogen bonds and van der Waals forces [19–21]. As a result, efficient decrystallization of cellulose to reorganize the inter- and intra-molecular network is a highly desirable process essential for cellulose modification.

Ionic liquids (ILs) mediated regeneration as the emerging green process for deconstruction of cellulose network has gained widespread acceptance [22] due to their low vapor pressure, property-tunability, and recyclability as green solvents. The regeneration of cellulose via ionic liquid dissolution could cause the structural rearrangement of cellulose in terms of crystalline structure and surface morphology, which influences the efficiency of following modification of cellulose

* Corresponding author at: Gustav Wieds Vej 10, 8000 Aarhus, Denmark.
E-mail address: guo@bce.au.dk (Z. Guo).

https://doi.org/10.1016/j.ijbiomac.2023.123983
Received 22 November 2022; Received in revised form 21 February 2023; Accepted 5 March 2023
Available online 10 March 2023

including TEMPO-mediated oxidation and succinylation [23–25]. The capacity of ILs to dissolve cellulose might be ascribed to successful breaking of inter- and intra-molecular hydrogen bonds presented in cellulose, where the anions and cations of ILs penetrate and interact with hydroxyl proton or oxygen, respectively as shown in Fig. S1. Imidazolium-based ionic liquids including 1-butyl-3-methylimidazolium hydrogen sulfate, 1-butyl-3-methylimidazolium chloride, and 1-ethyl-3-methylimidazole chloride were more classical ILs used for cellulose dissolution [25–27], due to their ease of production from low-cost starting materials with high yields. Not surprisingly, the dissolving capacity of chloride-anion paired ionic liquids decreased as the chain length of the cationic moieties increased ([C_4mim]Cl > [C_6mim]Cl > [C_8mim]Cl) [25–27]. Therefore, [C_4mim]Cl and [C_2mim]Cl were studied in this work.

Furthermore, TEMPO ((2,2,6,6-Tetramethylpiperidin-1-yl)oxyl)-mediated oxidation is one of the most studied methods to introduce carboxyl group and decrystallize cellulose [21]. In a typical TEMPO-NaClO-NaBr oxidation system, the hydroxyl groups at C6 of cellulose conversed into carboxyl groups. The negatively charged cellulose chains have a strong electronic repulsion, thus strengthening the delamination of cellulose [21]. Various functionalities containing hydrophilic groups and aromatic amino acid groups can be further added to delaminate cellulose after TEMPO-Mediated Oxidation [28–30]. However, the yield of water-soluble sodium oxidized cellulose from the TEMPO-mediated oxidation was generally very low (less than 10 wt%) [31], which limited its further applications. Some studies utilise the 4-acetamide-TEMPO/NaClO/NaClO2 system to produce a 20-33 wt% water-soluble fraction with high carboxyl content at pH 4.8. Comparable with the system at acid conditions [32–35], our hypothesis is that the assistance of ionic liquid mediated regeneration may overcome the low-yield problem for oxidation of cellulose, and even endow some enhanced properties to the oxidized cellulose.

In this work, the regeneration of cellulose by ionic liquids [C_4mim]Cl and [C_2mim]Cl as pre-treatment with (Two-step) or without (One-step) TEMPO-Mediated Oxidation post-treatment was investigated to depolymerize and functionalize cellulose. The resulting regenerated and oxidized celluloses were further functionalized via reaction with 2-dodecen-1-yl succinic anhydride (SAC12). This hydrophobic modification converted cellulose material into value-added emulsifiers that are effective for the delivery of nutritious ingredients or grease drugs, which presents a promising technology option for processing cellulose into highly functionalized materials for multi-purpose applications.

2. Materials and methods

2.1. Materials

Avicel® PH-101 cellulose (approx. particle size of 50 μm), 2, 2, 6, 6-tetramethylpiperidine 1-oxyl (TEMPO), (2,2′-azino-bis(3-ethylbenzothiazoline-6-sulfonic acid)), sodium bromide, sodium hypochlorite solution (10–15 % in water), 1-ethyl-3-methylimidazolium chloride [C_2mim]Cl and 1-Butyl-3-methylimidazolium chloride [C_4mim]Cl, 2-dodecen-1-yl succinic anhydride (SAC12) were purchased from Sigma-Aldrich (Søborg, Denmark). Refined bleached fish oil was procured from local supermarket. Other chemicals used as received were purchased from Sigma-Aldrich (Søborg, Denmark). The water used in this project was MilliQ water.

2.2. Preparation of pretreated celluloses

2.2.1. Preparation of regenerated cellulose (RC)

Avicel® PH-101 cellulose (0.5 g) was dispersed in 5 g ionic liquid, namely 1-ethyl-3-methylimidazolium chloride [C_2mim]Cl and 1-Butyl-3-methylimidazolium chloride [C_4mim]Cl at 90 °C for 4 h to produce regenerated cellulose, and then regenerated cellulose were washed by deionized water to remove the ionic liquids. To totally remove the ionic liquid, the dialysis of the regenerated celluloses pretreated by [C_2mim]Cl (RC2) and by [C_4mim]Cl was performed twice for 24 h each times. After dialysis, the final regenerated cellulose was dehydrated by freeze-drying for 72 h.

2.2.2. Preparation of TEMPO-mediated oxidized regenerated cellulose product (TRC)

Regenerated cellulose by [C_4mim]Cl (RC4)and [C_2mim]Cl (RC2)pretreatment (0.5 g) was dispersed in 500 mL water, followed by 0.25 g TEMPO (2,2,6,6-tetramethylpiperidine-1-oxyl radical) and 2.5 g sodium bromide (NaBr). Then, 33.2 mL of 37 % sodium hypochlorite solution (NaClO) was added to initiate the TEMPO-mediated oxidation. The reaction was kept running at pH 10 by continuous titration of 0.5 M sodium hydroxide (NaOH); until the pH of the reaction system remained unchanged (record the reaction time), 33.2 mL 96 % ethanol was then added to terminate the oxidation. After 10 min of centrifugation at 4000 rpm, the supernatant was collected and then poured into 500 mL ethanol to precipitate oxidized cellulose. After dialyzing for 24 h to remove unreacted TEMPO, NaBr, and NaClO, the final product of oxidized cellulose was freeze-dried for 72 h.

2.3. Characterization of depolymerized cellulose products (RC and TRC)

2.3.1. Confirmation of crystalline properties by X-ray powder diffraction (XRD)

Wide-angle X-ray diffraction (Shimatzu diffractometer, XRD 6100, Kyushu, Japan) was operated to examine the crystalline structures of the samples at 20 kV and 5 mA. The scanning angle range used for continuous scanning was 5–40°. The relative crystallinity derived from the crystallinity index (C_rI) can be calculated using the formula below (cellulose I: Eq. (1) [36], cellulose II: Eq. (2) [37])

$$C_r\mathrm{I} = \frac{I_{200} - I_{am}}{I_{200}} \times 100\% \quad (1)$$

$$C_r\mathrm{I} = \frac{I_{110} - I_{15}}{I_{110}} \times 100\% \quad (2)$$

where I_{200} and I_{110} is the diffractogram height of (200) peak or cellulose I, (110) peak for cellulose II in this study), and I_{am} and I_{15} is the height of the amorphous background ($2\theta = 19.0°$ for cellulose I, $2\theta = 15°$ for cellulose II in this study), respectively.

2.3.2. Confirmation of structure change of TRC by Fourier-transform infrared spectroscopy (FTIR)

FTIR spectra were recorded in absorbance mode in the range of 4000–650 cm^{-1} region at a resolution of 4 cm^{-1}, using a Q-interline QFAflex spectrometer (Trølløse, Denmark) equipped with a deuterium triglycine sulfate detector. The samples were mounted in their pure solid form in a Pike attenuated total reflectance (ATR) device at 25 °C, and the spectra were ratioed against a single-beam spectrum of the clean ATR crystal.

2.3.3. Degree of oxidation (DO) of TRC

The degree of oxidation was determined by using a complex metric titration with EDTA reported by Zhang et al. [38] with some modifications. The TOC was weighed (200 mg) and suspended in 40 mL MilliQ water in a 100 mL flask. 20 mL 1 % $CuSO_4$ solution was added and then stirred at 400 rpm for 30 min. After centrifugation at 4000 rpm for 10 min, the precipitant was collected. Then the precipitant was dissolved or suspended in 8 ml MilliQ water with the addition of 1 mL 5 % aqueous ammonia solution.

A mixture of murexide: NaCl (1:90) as the indication of titration was added and 0.01 M EDTA solution was used to subsequently titrate with tetra ammine copper complexion. When the color is changed from orange to purple and kept being purple, the titration should be stopped.

The degree of oxidation was calculated according to:

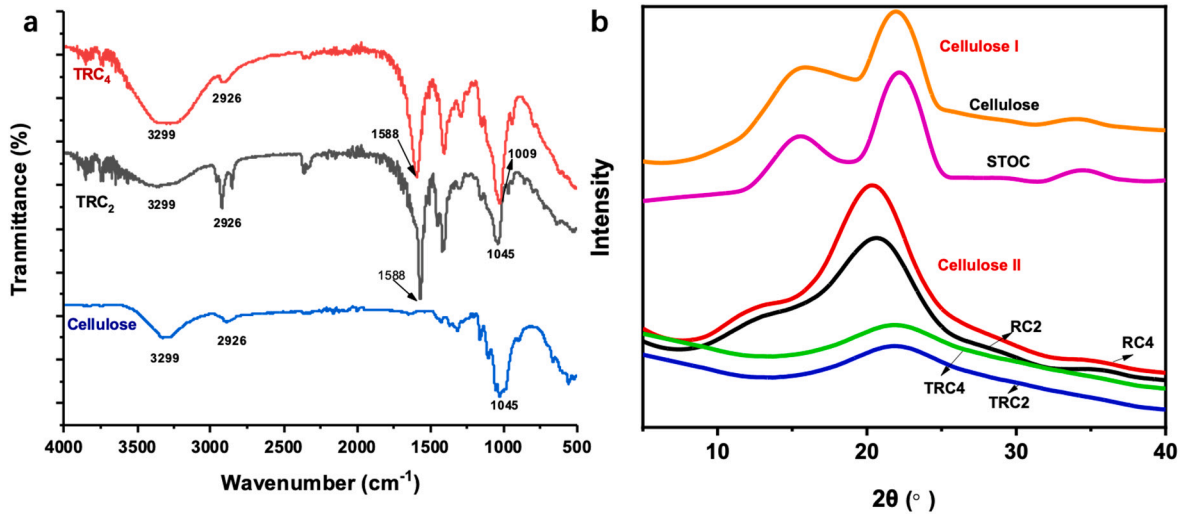

Fig. 1. a). FTIR spectra of cellulose, tempo-mediated oxidized regenerated cellulose by [C_2mim][Cl] and[C_4mim][Cl](TRC2, TRC4); b) X-ray diffraction curves of Cellulose, Regenerated cellulose by [C2mim][Cl] and [C4mim][Cl](RC2 and RC4), tempo-mediated oxidized Cellulose(STOC), tempo-mediated oxidized regenerated cellulose by [C2mim][Cl] and[C4mim][Cl] (TRC2 and TRC4).

$$DO = \frac{162*2*V*c*f}{m - 36*2*V*c*f} \times 100$$

where V is the used volume of EDTA solution, c is the concentration of EDTA solution, f is the factor of the EDTA solution, and m is the weight of ITOC. 36 is the molar mass difference of carboxyl cellulose and 162 is the molar mass of an anhydroglucose unit.

2.3.4. Scanning electron microscopy (SEM) of RC and TRC

The SEM images of all samples were taken with a Hitachi TM3030PLUS TABLETOP MICROSCOPE (Japan) at a voltage of 20 kV and a magnification of (200) and (800).All samples were freeze-dried before being measured.

2.4. Preparation of alkyl/alkenyl succinylated RC-based or TRC-based products

The RC [39] or TRC was succinylated with 2-dodecen-1-yl succinic anhydride (SAC12) with inspiration from a previously reported method [14]. 99 mg TRC or 81 mg RC was dispersed or dissolved in 10 mL water in 15 ml glass vials, followed by the addition of 932 mg SAC12. During the reaction, the pH was adjusted continuously to maintain at 7.00 ± 0.1 using 0.1 M NaOH. After 4 h, centrifugation at 4000 rpm for 10 min at 20 °C was performed to collect the supernatant. After freeze-drying for 48 h, 40 ml acetone was added to the dried samples to remove the remaining SAC12. The final product was obtained after removal of acetone at room temperature for 24 h.

2.5. Characterization of succinylated RC-based or TRC-based products

2.5.1. Confirmation of succinylation by FTIR

FTIR spectra were recorded in absorbance mode in the 4000–650 cm^{-1} region at a resolution of 4 cm^{-1}, using a Qinterline QFAflex spectrometer equipped with a deuterium triglycine sulfate detector. The samples were mounted in their pure solid form in a Pike attenuated total reflectance (ATR) device at 25 °C, and the spectra were ratioed against a single-beam spectrum of the clean ATR crystal.

2.5.2. Static drop shape analysis

Contact angle measurements using static axisymmetric drop shape mode were done to assess the interfacial tension-lowering impact of samples including RC2-SAC12, RC4-SAC12, TRC2-SAC12, TRC4-SAC12. Oil was dropped on the glass surface to produce an oil surface for two days. A Krüss DSA10 goniometer was used to investigate the contact angles of drops (10 ± 1 μL) of an aqueous solution of a sample with 0.3 wt% concentration on the oil surface. The surface-drop contact angles were determined approximately 15 s after the drops were placed on the non-polar oil surface. The contact angles were measured at room temperature with three determinations for each sample.

2.5.3. Scanning electron microscopy (SEM)

The SEM images of all samples were taken using a Hitachi TM3030PLUS TABLETOP MICROSCOPE (Japan) at a voltage of 20 kV and a magnification of (200) and (800). All samples were freeze-dried before being measured.

2.6. Application of succinylated compounds in oil-in-water emulsions

RC2-SAC12, RC4-SAC12, TRC2-SAC12, and TRC4-SAC12 were dissolved in water as an aqueous fraction and were mixed with 10 wt% fish oil. To fabricate the emulsion, they were ultrasonically homogenized in an ice bath for 5 min with 4 cycles and 57 % power using a high-intensity ultrasonic cell disruptor (UW 2200, BANDELIN SONOPULS). To prevent microorganisms from growing at room temperature, 0.02 wt% sodium azide was added.

2.6.1. Confocal laser scanning microscopy (CLSM)

The droplet dispersion of the emulsions was visualized via confocal laser scanning microscopy (Zeiss LSM780). To photograph the lipid phase and aqueous phase, 1 mL emulsions were mixed with Nile red solution (10 L, 1 mg/mL in acetone) and Rhodamine 6G (10 L, 1 mg/mL in water). The fluorescence emission intensity of Nile red and Rhodamine 6G molecules was collected across 539–753 nm for Nile red molecules and over 517–696 nm for Rhodamine 6G molecules, respectively. Zeiss LSM Image Browser software was used to analyze the images.

2.6.2. Emulsion characteristics (average droplet size)

At 25 °C, Zetasizer Nano ZS (Malvern Instruments, Worcestershire, UK) was used to assess particle size. The emulsions were diluted with deionized water (1:500). DLS measured the size distribution of emulsion droplets via non-invasive backscatter optics. Three measurements were analyzed separately.

Table 1
Characterization of TEMPO-Mediated oxidized cellulose products (Tempo-mediated oxidized Cellulose (STOC), TEMPO-mediated oxidized Regenerated cellulose by [C_2mim][Cl] (TRC2) and [C_4mim][Cl] (TRC4).

	Reaction time (h)	Carboxylated content (mmol COO^-/g)	Degree of oxidation (%)	Yield (%)
TRC_2	1.81 ± 0.60	3.23 ± 0.07	59 ± 0.01	45.30 ± 6.79
TRC_4	1.18 ± 0.36	3.42 ± 0.06	62.3 ± 0.02	46.55 ± 1.91
STOC	3.90 ± 0.21	2.00 ± 0.28	35 ± 5.26	4.04 ± 0.04

Table 2
Crystallinity index of cellulose and depolymerized cellulose including TEMPO-mediated oxidized Cellulose (STOC), Regenerated cellulose by [C_2mim][Cl] (RC2) and [C_4mim][Cl] (RC4), and Tempo-mediated oxidized Regenerated cellulose by [C_2mim][Cl] (TRC2) and [C_4mim][Cl] (TRC4).

Samples	Crystallinity Index(%)
Cellulose	71.1
STOC	58.47
RC2	46.64
RC4	53.19
TRC2	37.11
TRC4	39.28

2.7. Antioxidant activity

2.7.1. ABTS radical scavenging

To evaluate the ability of samples to scavenge ABTS (2,2′-azino-bis (3-ethylbenzothiazoline-6-sulfonic acid)) radicals (ABTS*), an analysis was performed according to Li et.al [40]. By combining equal amounts of 7 mM ABTS and 2.45 mM $K_2S_2O_8$ in deionized water, followed by a 24-h dark incubation, it was achievable to partially oxidize ABTS using $K_2S_2O_8$. After diluting the resulting ABTS* solution in deionized water, the final absorbance measured at A_{734}nm was 0.7000 ± 020. Samples were dissolved in water to a concentration of 25 mg/mL.50 mL of this solution was then carefully mixed with 1 mL of ABTS* solution. The decrease in absorbance at 734 nm was detected throughout a 30-min period at room temperature. The equation ABTS Scavenging(%) = $(A_{INITIAL} - A_s) / A_{INITIAL} * 100$ % was used to calculate the percentage of ABTS* that was scavenged. INITIAL stands for the absorbance at the beginning of the reaction ($A_{734nm} = 0.7000.020$), and AS stands for the absorbance after a specific amount of time with a specific concentration of saccharide. For each sample, two sets of spectrophotometric data were collected and two sets of samples were analyzed.

2.7.2. Ferrous chelating ability test

Iron chloride (3 mM), ferrozine (3 mM), and 300 μL of the sample solution were combined for the Fe^{+2} chelating activity experiment [41]. The absorbance was taken at 562 nm after 10 min. In place of the sample solution, 300 μL of water was used to create the control sample. The formula used to determine the amount of Fe^{+2} chelating activity is as follows: Fe^{+2} chelating activity (%) = $(A_c - A_s) * 100 / Ac$, where A_c is the absorbance of the control and As is the absorbance of the sample.

3. Results and discussion

3.1. Characterization of regenerated cellulose (RC and TRC)

3.1.1. Characterization of oxidized TRC

TEMPO-mediated oxidized regenerated cellulose by ionic liquids (TRC2 and TRC4) was characterized by FTIR, carboxyl content, degree of oxidation, SEM, and XRD. The selective oxidation of alcoholic hydroxyls on cellulose bone into carboxylate groups at the C6 position was effectively catalyzed by TEMPO as shown in Fig. S2 [42], evidenced by change of FTIR absorption peaks. In the FTIR spectra of TRC2 and TRC4 (Fig. 1a), the obvious peak at 1588 cm^{-1} appeared, compared with cellulose's spectrum. It is assigned as the C═O stretching vibration of carboxylate groups [43–45].The carboxyl content and degree of oxidation of TRC2 and TRC4 were determined by NaOH titration, and Soluble TEMPO-mediated oxidized cellulose (STOC) without ionic liquid pretreatment was studied as a comparison (Table 1). STOC presented 35 % of the degree of oxidation and 2.00 mmol COO^-/g of the carboxylate content. The carboxyl content and the degree of oxidation was quite higher than the values in other studies of different TEMPO systems (lower than 1.7 mmol/g) [31,42,46,47], which may contribute to the higher NaClO dosage in the reaction [48]. After ionic liquid pretreatment, the carboxylate content enhanced significantly, namely, 3.23 mmol COO−/g (TRC2) and 3.42 mmol COO−/g (TRC4). Encouragingly, the degree of oxidation (59–62 %) enhanced 1.7 times compared to the one of STOC without ionic liquid pretreatment (35 %). This may contribute to IL-mediated depolymerization or inter-chain dissociation, including decreased molecular weight, decreased crystallin index and depolymerized structure; which make the cellulose molecules more accessible to TEMPO oxidation reagent. The enhanced carboxylate contents could endow TRC2 and TRC4 with strong electrostatic repulsion between charged cellulose chains, thereby facilitating the delamination of cellulose [42,49–51]. In addition, β-eliminations and the effects of the cleavage unit of anhydroglucose induced by hydroxyl or other active radicals during the oxidation may also promote cellulose delamination [52,53].

Another thing worth mentioning is the increased water-soluble fraction product yield after the ionic liquid dissolution regeneration. The yield of water-soluble fabrication from the TEMPO-mediated oxidation was generally very low (4.04 ± 0.04 %) based on the original cellulose [31], which limited its further applications. The high-crystalline structure of cellulose with high molecular weight (39,000 g/mol, data provided by Sigma-Aldrich) and high crystalline index made cellulose chains hard to access by the oxidant reagent and produced more water-insoluble fractions with high-crystallin structure. For IL-regenerated cellulose, up to 46.55 ± 1.91 % (RC2) and 46.55 ± 1.91 (RC4) yield of water-soluble fractions were achieved. Compare with the reported high water-soluble fraction yield achieved by other methods, such as 20-33 wt% in 4-acetamide-TEMPO/NaClO/NaClO2 system [32–35], ionic liquid-mediated regeneration achieved a even higher yield, which may be ascribed to the penetration and depolymerization by ILs, resulting in changes of molecular weight, morphology, and crystalline index. Some of cellulose molecules may be degraded to short molecules during by IL interaction and dissociation [16,54]. The crystalline index significantly decreased (Fig. 1 and Table 1), and more amorphous broken structures in the morphology image observed (Fig. 3). Besides, the shortened oxidation reaction time of regenerated cellulose (1.81 ± 0.60 h or 1.18 ± 0.36 h), compared with the one of cellulose (3.90 ± 0.21 h), could save the reaction time in practical industrial applications.

3.1.2. XRD of RC and TRC

High crystalline structure of cellulose, as well as strong intermolecular and intramolecular hydrogen bonding, are thought to be responsible for its innate resistance to subsequent succinylation modification [55]. Fig. 1b and Table 2 illustrated the possible change of the crystalline structure after several decrystallization processes. Basically, the cellulose crystal I exist in nature cellulose without any treatment, whereas the crystal pattern of cellulose may change depending on different treatments. Crystal I (with twice the hydroxymethyl group conformation and two intramolecular hydrogen bonds along the glycosidic linkage) is made up of parallel chains of hydrogen-bonded sheets that stack on top of each other due to van der Waals interactions, whereas Crystal II (with twice the hydroxymethyl group

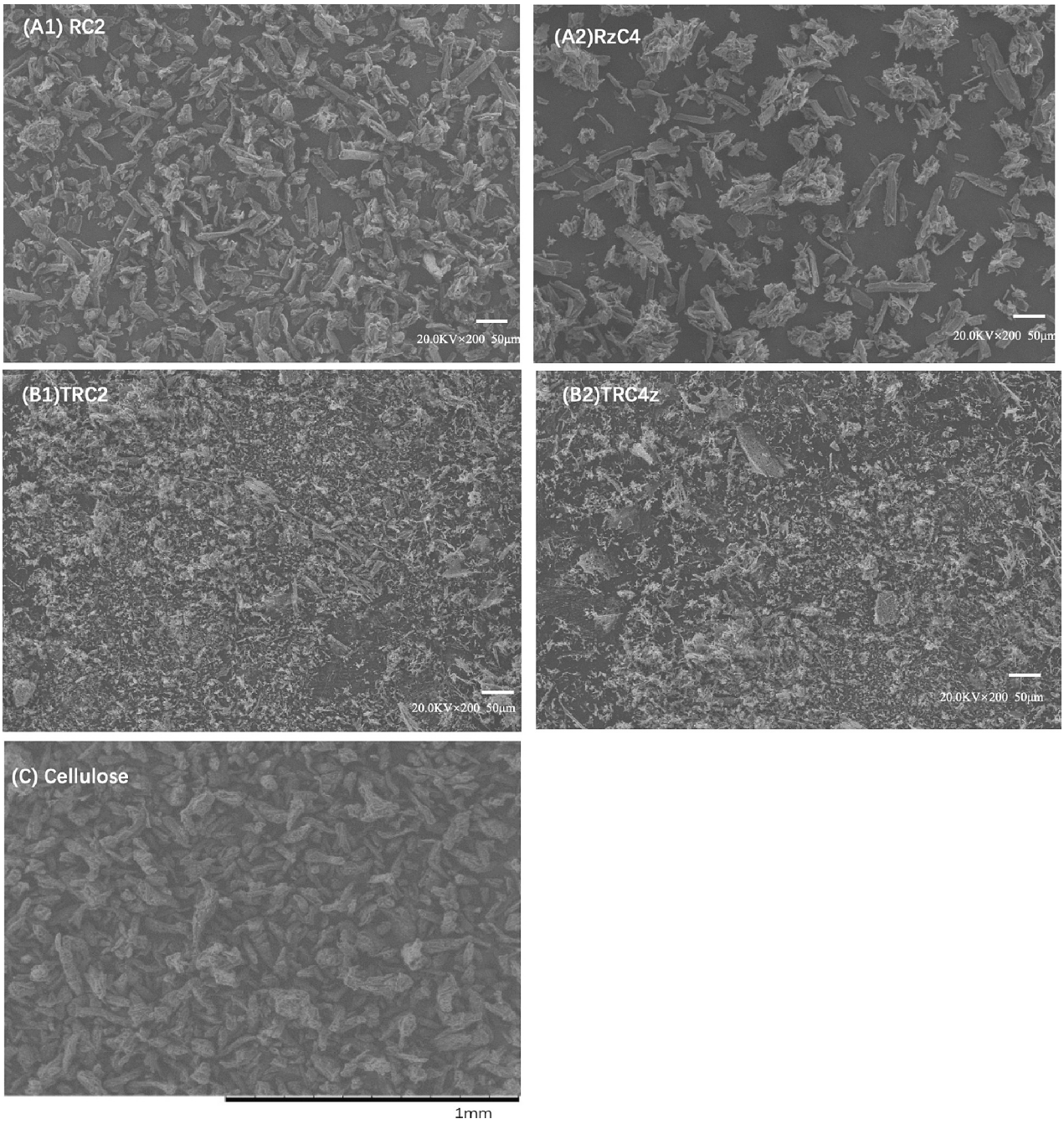

Fig. 2. SEM micrographs of the original cellulose (Avicel PH-101) without pretreatment (C) cited from previous work, and the solids obtained after pretreatment with different treatments: (A)Regenerated cellulose by [C2mim][Cl] (RC2) and[C4mim][Cl] (RC4), (B)Tempo-mediated oxidized Regenerated cellulose by [C2mim][Cl] (TRC2) and [C4mim][Cl] (TRC4). The panel depicts the samples at lower magnification (200).

conformation and only one intramolecular hydrogen bonds along the glycosidic linkage) consists of antiparallel chains which is less thermodynamical stable than Crystal I, resulting in being much easier process for further reaction [41]. Both Celluloses I crystal and Cellulose II crystal have characteristically diffraction peaks: as for Cellulose I crystal, $2\theta = 14.8°$, $16.4°$, $22.6°$, and $34.2°$ are indexed as ($11\bar{0}$), (110), (200), and (040) planes; as for Cellulose II crystal, peaks at $2\theta = 12.3°$, $20.2°$, and $21.9°$ are the characteristic of ($11\bar{0}$), (110), and (200) planes. From Fig. 1b, it is obvious that raw cellulose without any treatments which had $13.07°$ ($11\bar{0}$), $21.67°$ (200), $34.2°$ (040) overlapped partially, was assigned to Cellulose I. After ionic liquid dissolution and regeneration, an expected transformation of Cellulose I to Cellulose II crystalline structure was achieved with peaks at $12.3°$ and $20.2°$ responding to ($11\bar{0}$) and (110) of Cellulose II detected, together with the slight crystallinity index change, which may benefit further reactive succinylation. On the other hand, TEMPO-mediated oxidation made no change about the crystalline structure and small crystallinity index change. As for the TRC2 and TRC4 with TEMPO-mediated oxidation and IL pretreatment, only one broad peak at $21.9°$ ((200) planes of cellulose II) was detected, and such changes imply that cellulose I completely transformed to cellulose II following the regeneration process. The XRD patterns of the amorphous cellulose agree with previous research in the literature and a great decrease in the crystalline index was achieved from 71.1 % (cellulose) to 37.11 % or 39.28 % (TRC2 and TRC4, respectively). Overall, Ionic Liquid treatment is an effective method to convert Cellulose I into Cellulose II crystalline structure, compared with

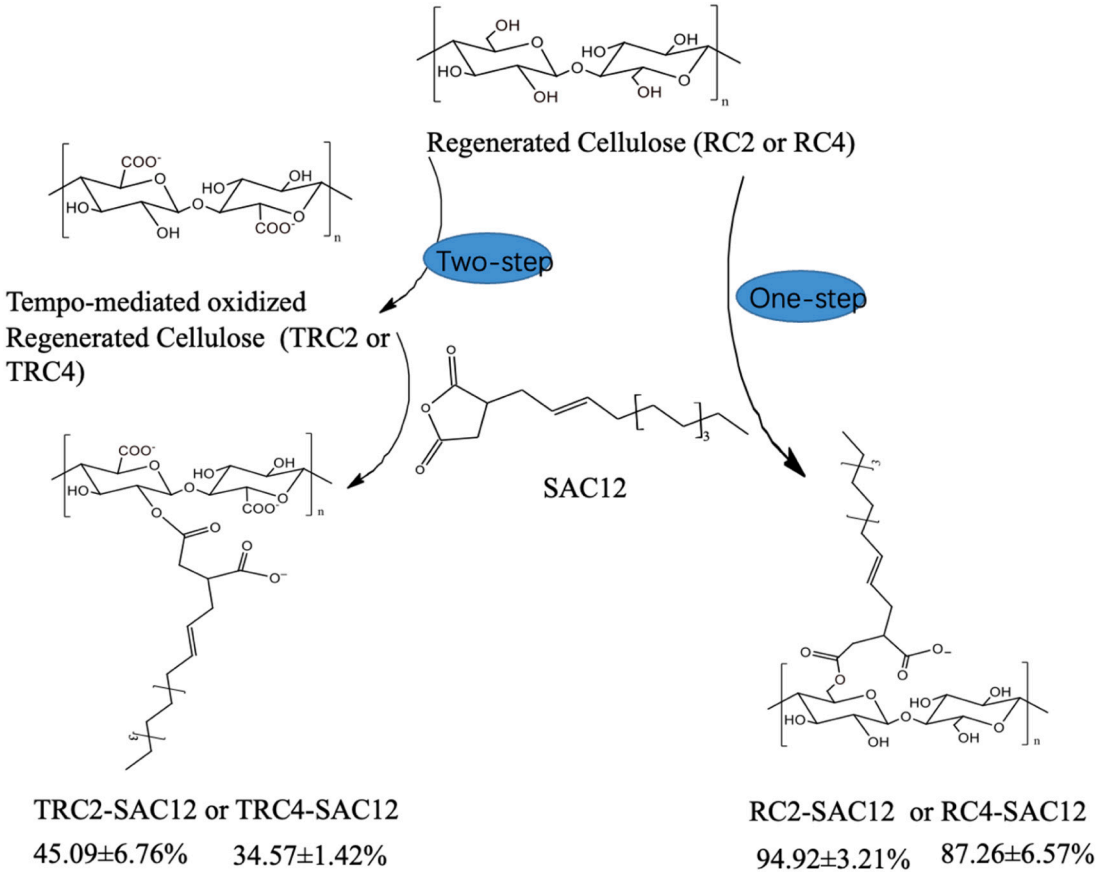

Fig. 3. The reaction scheme of Succinylation of Regenerated cellulose by [C_2mim][Cl] (RC2-SAC12) and [C_4mim][Cl] (RC2-SAC12) pre-treatments, and Tempo-mediated oxidized Regenerated cellulose by [C_2mim][Cl] (TRC2-SAC12) and [C_4mim][Cl] (TRC4-SAC12).

TEMPO-mediated oxidation, which could affect the subsequent modification.

3.1.3. Scanning electron microscopy (SEM) of RC and TRC

The morphology of the pretreated cellulose samples with ionic liquid dissolution regeneration together TEMPO-Mediated Oxidation or not was examined by SEM, shown in Fig. 2. The micrographs in the right part (C) of the Fig. 2 show the original cellulose without pretreatment, which was cited from previously published work. After ionic liquid dissolution regeneration, the aggregated cellulose molecules are slightly looser and less tightly arranged compared with the original cellulose from lower magnification. Besides, under the TEMPO-Mediated Oxidation treatment, TRC materials had a more broken structure, which could easily explain the significant decrease in the crystalline index. It may result from the TEMPO-mediated Oxidation that could distribute the amorphous region of cellulose.

3.2. Characterization of succinylated RC or TRC

The alkyl/alkenyl succinylation of regenerated cellulose (RC2 and RC4), and TEMPO-mediated oxidized regenerated cellulose (TRC2, TRC4) was schematically presented in Fig. 3. From the starting materials (cellulose) to the final succinylated products, the product yields synthesized using various decrystallization methods were significantly different, namely two-step decrystallizations IL-regeneration-coupling-TEMPO-mediated oxidation: 45.09 ± 6.76 % for TRC2-SAC12, 34.57 ± 1.42 % for TRC4-SAC12, and One-step decrystallization IL-regeneration: 94.92 ± 3.21 % for RC2-SAC12, 87.26 ± 6.57 % for RC4-SAC12, respectively. The lower succinlyation product yield from the two-step decrystallization was due to the reason that some insoluble fractions were discarded after TEMPO-Mediated Oxidation. But only focus on the succinylation step, the yields and reaction efficiencies are almost same (94.27 ± 7.45 wt% for TRC2-SAC12, 91.09 ± 1.28 wt% for TRC4-SAC12, 94.00 ± 1.29 wt% for RC2-SAC12, 93.45 ± 0.91 wt% for RC4-SAC12).

The fraction of succinylated products with alkyl/alkenyl succinyl group incorporated into cellulose-based materials was proved by FTIR analysis. Due to the incorporation of the alkyl/alkenyl succinyl anhydride group, the increased hydrophobicity of samples was proved by the decrease of contact angle on a hydrophobic surface, which will benefit stabilization of oil-in-water emulsion. The related discussion is detailed in the following section.

3.2.1. Fourier transform infrared spectroscope (FTIR)

The FTIR spectra of succinylated cellulose products including TRC_4-SAC12, TRC_2-SAC12, RC_4-SAC12, RC_2-SAC12 exhibited in Fig. S3. The unmodified cellulose and SAC12 were investigated as a comparison. 3299, 2891, 1308, 1023 and 894 cm^{-1} are associated with untreated cellulose marked in yellow. The significant absorption at 3299 cm^{-1} is caused by the stretching of O—H groups, whereas the one at 2891 cm^{-1} is assigned to the stretching of C—H groups. The band at 1308 cm^{-1} arises from the O—H bending. The absorption band at 1161 cm^{-1} relates to C—O stretching in celluloses. A high peak at 1023 cm^{-1} was generated by C-O-C pyranose ring skeletal vibration (Sun, et al., 2004b). A sharp band at 894 cm^{-1} indicated the β-glucosidic linkages between the sugar units (Gupta, Madan, & Bansal, 1987). 1857 and 1781 cm^{-1} are the characteristic peaks of two anhydride carbonyl bands of succinic anhydride SAC12, whereas 2919 cm^{-1} respected alkane moieties of the substitutions. Different from cellulose and SAC12, two new peaks (1710 and 1571 cm^{-1}) were generated in all succinylated products' spectra

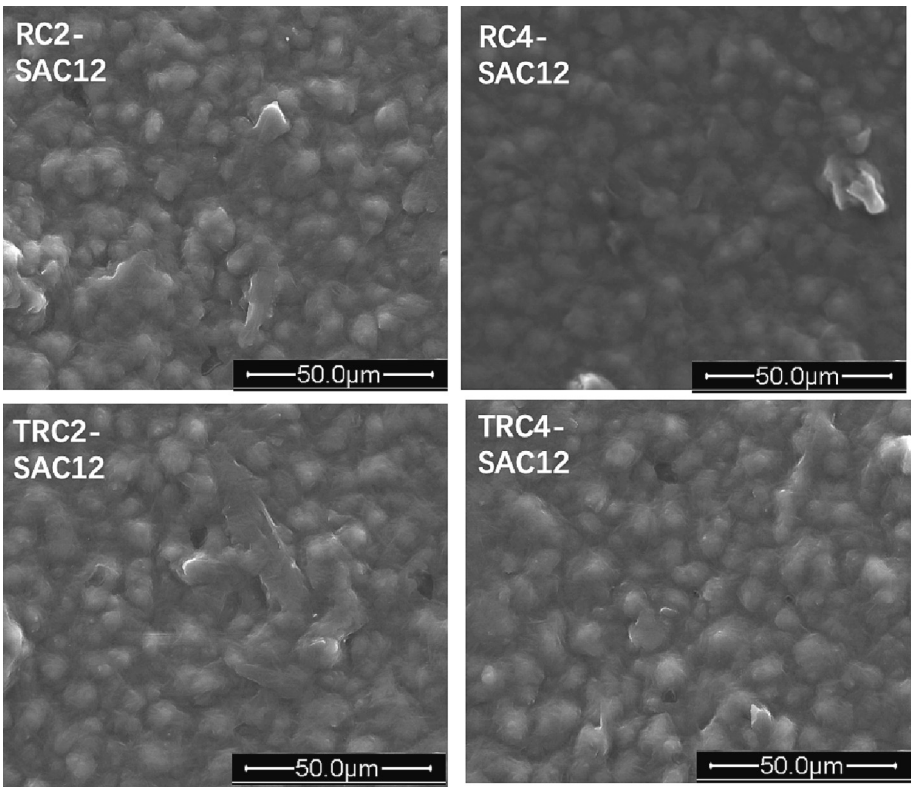

Fig. 4. SEM of Succinylation of Regenerated cellulose by [C2mim][Cl] (RC2-SAC12) and [C4mim][Cl] (RC2-SAC12) pre-treatments, and Tempo-mediated oxidized Regenerated cellulose by [C2mim][Cl] (TRC2-SAC12) and [C4mim][Cl] (TRC4-SAC12).

demonstrating the achievement of succinylation. The band at 1710 cm^{-1} is indicative of absorption by the ester bonds between cellulose compounds and succinic anhydride. The band at 1567 cm^{-1} is due to the C—O asymmetric stretching vibrations of carboxylic anions (Yoshimura, Matsuo, & Fujioka, 2006). On the other hand, the peak at 2919 cm^{-1} was generated compared with unmodified cellulose, which was also appeared in SAC12, representing the alky succinic group was linked to cellulose and the succinylation was processed successfully as expected.

3.2.2. Contact angle

Determination of interfacial capability of stabilizer at the water-oil interface is useful for understanding the emulsifying property of an ingredient. The contact angle (Fig. S4) was investigated, which could indicate the hydrophilicity/hydrophobicity of the samples, the efficiency of adsorption, and coverage of samples around the oil droplet in the water phase [56]. After TEMPO-mediated oxidation, TRC2 and TRC4 exhibited high contact angles with more than 90°, showing strong hydrophilicity. However, after alkyl/alkenyl succinylation, the contact angles of all the succinylated samples (RC2-SAC12, RC4-SAC12, TRC2-SAC12, TRC4-SAC12) decreased to lower than 35°. Alkyl/alkenyl succinylation, which incorporates hydrophobic group into the cellulose-based samples including RC2, RC4, TRC2, TRC4, increase the hydrophobicity significantly. All the succinylated pretreated samples containing both hydrophobic group (alkyl/alkenyl succinyl group) and hydrophilic group (hydroxyl group on the cellulose backbone) have a lower contact angle, which gives the sample better wetting properties, compared with the alkyl/alkenyl succinylated cellulose without any pretreatment [14,57]. The amphiphilicity may be the main driving force for stabilizing the oil-in-water emulsion [58], being the stabilizer could be adsorbed on the surface of the oil droplet, thus forming a protective physical barrier layer [14,57]. The homogenous succinylated materials, shown in Fig. 4 also benefit the interface behavior. Besides, compared with the Cellulose-SAC12, the pretreatment before the succinylation reaction could lower the contact angle of the succinylated products RC2-SAC12 and RC4-SAC12, which indicated the more hydrophilic OH group was exposed by IL-pretreatment.

3.2.3. Scanning electron microscopy (SEM)

The morphologies of alkyl/alkenyl succinylated regenerated cellulose by [C2mim][Cl] (RC2-SAC12) and [C4mim][Cl] (RC2-SAC12) pretreatments, and TEMPO-mediated oxidized regenerated cellulose by [C2mim][Cl] (TRC2-SAC12) and [C4mim][Cl] (TRC4-SAC12) were measured by SEM (Fig. 4). Compared with the image of materials without succinylation, more homogenous circle particles were formed, which might be due to a better adsorption of alkyl/alkenyl succinylated materials on the surface of the oil droplet through hydrophobic interaction, and then aligned on the surface of the oil droplet.

3.3. Application of succinylated celluloses in oil-in-water emulsions

3.3.1. Emulsion characteristics

In general, nanocellulose could be utilized for stabilizing oil droplets in the Pickering emulsion [59], however, due to the super hydrophilicity of TRC2 and TRC4, they cannot be available to coat the oil droplet and fabricate the homogeneous emulsion system, shown in the Fig. S5. After succinylation of either regenerated cellulose or TEMPO-mediated oxidized regenerated cellulose, the amphiphilicity should be entitled to all succinylated cellulose-based samples, which could be more applicable to the fabrication and stabilization of O/W emulsion systems. The average droplet sizes of the fish oil-in-water emulsion stabilized by TRC2-SAC12, TRC4-SAC12, R2-SAC12, and RC4-SAC and their changes for 8 weeks storage period were shown in Fig. 5a. The average droplet sizes of emulsion stabilized by all the succinylated samples were insignificantly different, with 171.53 ± 2.06 nm (TRC2-SAC12), 168.3 ± 0.46 nm (TRC4-SAC12), 181.9 ± 2.55 nm (R2-SAC12), 175.2 ± 2.00 nm (RC4-SAC12), respectively. Even after 8 weeks' storage, the corresponding emulsions remain almost unchanged in average droplet size, indicating their superior stability. Furthermore, it demonstrated that

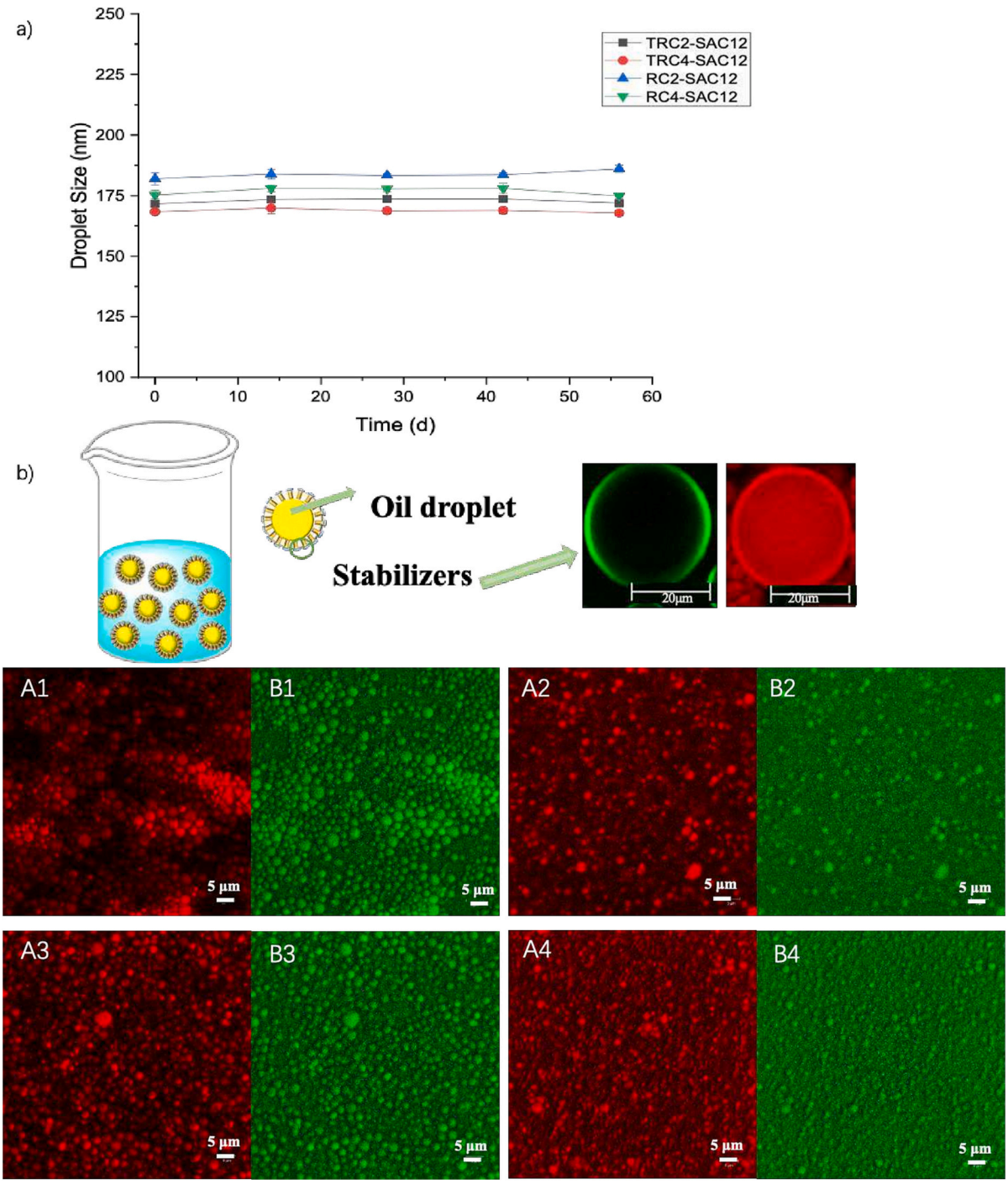

Fig. 5. a). The droplet size of emulsions with 10 wt% oil stabilized by 0.9 wt% compounds including RC2-SAC12, RC4-SAC12 and TRC2-SAC12, TRC4-SAC12 within 8 weeks; b). The CLSM image of the emulsions containing 10 wt% fish oil stabilized by different compounds with 0.9 wt% concentration. Images in A1, A2, A3, A4 show the oil phase stained with Nile Red (red). The aqueous phase shown in B1, B2, B3, B4 were stained with Rhodamine 6G (green). A1 and B1: RC2-SAC0; A2 and B2: TRC-SAC12; A3 and B3: RC4-SAC12; A4 and B4:TRC4-SAC12.

ionic liquid pretreatment was an effective method to enable succinylation of cellulose even without TEMPO-mediated oxidation, which exhibited a great ability to stabilize the emulsion. According to the XRD analysis data, the crystalline structure change (from cellulose I into cellulose II) caused by ionic liquid dissolution makes hydroxyl groups more accessible for alkyl/alkenyl succinylation of cellulose, whereas TEMPO-mediated oxidation did not result in such a significant change in structure. The succinylated pretreated-cellulose chains first adsorbed on the surface of the oil droplet through hydrophobic interaction, and then gradually aligned on the surface of the oil droplet, which could be confirmed from the enlarged CLSM image of one droplet in Fig. 5b. The significant electronic repulsion between the droplets coated by the highly negatively charged succcinylated pretreated-cellulose products (shown in Table S1), also contributed to the high stability of the emulsion. The uniform droplet distribution of the emulsions using alkyl/alkenyl succinylated celluloses was visualized in Fig. 5b, which further confirmed the excellent emulsifying capability of synthesized novel emulsifiers.

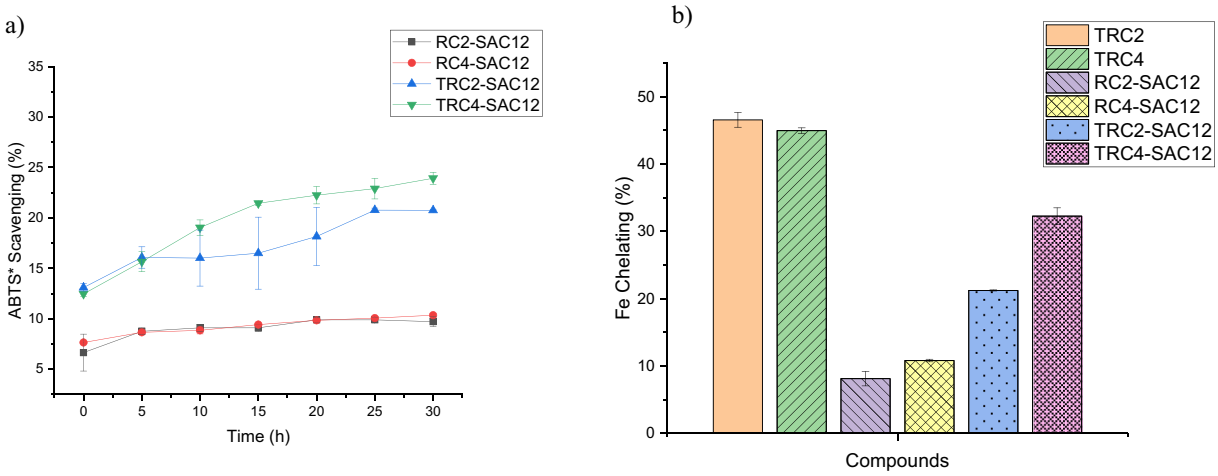

Fig. 6. The ABTS * Scavenging ability (a) and Fe^{2+} Chelating ability (b) of Succinylated Regenerated cellulose by [C_2mim][Cl] and[C_4mim][Cl] (RC2-SAC12, RC4-SAC12), and Succinylated Tempo-mediated oxidized Regenerated cellulose by [C_2mim][Cl] and[C_4mim][Cl] (TRC2-SAC12, TRC4-SAC12).

3.4. Antioxidant activity

Fig. 4a exhibited the ABTS radical scavenging ability of a series of succinylated cellulose-based products including succinylated regenerated cellulose by [C_2mim][Cl] and [C_4mim][Cl] (RC2-SAC12, RC4-SAC12), and succinylated TEMPO-mediated oxidized regenerated cellulose by regenerated cellulose [C_2mim][Cl] and[C_4mim][Cl]. TRC2 and TRC4 had no obvious ABTS radical scavenging capacity, which is consistence with the other results [60], therefore they were not shown in Fig. 6. From Fig. 6a, it is obvious that the scavenge ABTS* abilities of TRC2-SAC12 and TRC4-SAC12 was higher the those of RC2-SAC12 and RC4-SAC12. In general, the mechanism of reducing ABTS radicals is caused by the quenching effect of -OH or -COOH in succinylated oxidized celluloses in radical propagation reactions. Therefore, it can be inferred that TRC2-SAC12 and TRC4-SAC12, as compared to other non-oxidized celluloses (RC2-SAC12 and RC4-SAC12), possess higher radical quenching activity (2.2–2.4 times), which may contribute to the high carboxyl group and hydroxyl group content in TRC2-SAC12, TRC4-SAC12. Not surprisingly, RC2-SAC12 and RC4-SAC12 with less -COOH group resulted in lower scavenge ABTS* ability, which implied carboxyl group could increase much higher ABTS* scavenging ability of cellulose materials compared with the hydroxyl group. For Fe^{2+} chelating ability, non-alkyl/ono-alkenyl succinylated celluloses (TRC2 and TRC4) displayed significant higher activity, compared to alkyl/alkenyl succinylated celluloses as shown in Fig. 6b; which might be ascribed to higher hydrophobicity of alkyl/alkenyl succinylated celluloses. TRC2-SAC12 (22 %) and TRC4-SAC12 (35 %) also possessed a higher ability than RC2-SAC12 (8 %), and RC4-SAC12 (10 %); which likely can be attributed to high -COO^- group contents, resulted from TEMPO-mediated oxidation. High-density of -COOH groups in TRC2-SAC12 and TRC4-SAC12 could more effectively chelate Fe^{2+} by strong coordinating effect. Both ABTS* scavenging ability and Fe^{2+} chelating capability are preferable properties of antioxidants. Either IL-pretreatment, TEMPO-mediated oxidation or alkyl/alkenyl succinylation could produce desirable properties, which could increase the likelihood of reducing lipid oxidation when employed as building cell materials of delivery cargo and protecting oxidation-sensitive nutrients. In brief, IL-pretreatment coupling with TEMPO-mediated oxidation and sequential succinylation could be the best recommendation to synthesize cellulose-based emulsifiers for multi-purpose applications as emulsifier, stabilizers and antioxidants.

4. Conclusion

This work demonstrated that pretreatment of cellulose by hydrophilic ionic liquids can be an effective strategy to decrystallize and restructure cellulose (leading to the crystalline structure change of cellulose from crystalline I to crystalline II). IL-mediated decrystallization can greatly improve the reactivity and accessability of cellulose to oxidant such as TEMPO specie; thus improving the reaction efficiency. The proved that IL-regenerated cellulose can be directly alkyl/alkenyl succinylated without TEMPO-mediated oxidation. This work also demonstrated multi-step processes, IL-mediated regeneration and TEMPO-mediated oxidation, coupling with alkyl/alkenyl succinylation could be a preferable strategy; yielding the product having excellent ABTS* scavenging ability and Fe^{2+} chelating properties which could find extensive application in multi-sector industries.

CRediT authorship contribution statement

Ziqian Li: Conceptualization, Methodology, Writing - Original Draft, Investigation.

Guoqiang Zhang: Methodology and Investigation.

Dimitris Charalampopoulos: Supervision.

***Zheng Guo:** Conceptualization; Supervision, Writing: review and correction, and Funding acquisition.

Declaration of competing interest

The authors declare that they have no known competing financial interests or personal relationships that could have appeared to influence the work reported in this paper.

Data availability

Data will be made available on request.

Acknowledgement

Financial supports from Danmarks Frie Forskningsfond | Teknologi og Produktion (0136-00206B) and the Novo Nodisk Fonden (NNF16OC0021740) are gratefully acknowledged. Ziqian Li thanks the China Scholarship Council for its financial support for her Ph.D. study at Aarhus University, Denmark.

Appendix A. Supplementary data

Supplementary data to this article can be found online at https://doi.org/10.1016/j.ijbiomac.2023.123983.

References

[1] S. Acharya, Y. Hu, N. Abidi, Cellulose dissolution in ionic liquid under mild conditions: effect of hydrolysis and temperature, Fibers 9 (1) (2021) 5, https://doi.org/10.3390/fib9010005.

[2] P. Li, S. Wang, S.X. Zhou, Pickering emulsion approach for fabrication of waterborne cross-linkable polydimethylsiloxane coatings with high mechanical performance, J. Colloid Interface Sci. 585 (2021) 627–639, https://doi.org/10.1016/j.jcis.2020.10.042.

[3] A. Marefati, B. Wiege, N.U. Haase, M. Matos, M. Rayner, Pickering emulsifiers based on hydrophobically modified small granular starches - part I: manufacturing and physico-chemical characterization, Carbohydr. Polym. 175 (2017) 473–483, https://doi.org/10.1016/j.carbpol.2017.07.044.

[4] H.A. Fonseca-Florido, H.G. Vazquez-Garcia, G. Mendez-Montealvo, U.A. Basilio-Cortes, R. Navarro-Cortes, M.L. Rodriguez-Marin, J. Castro-Rosas, C.A. Gomez-Aldapa, Effect of acid hydrolysis and OSA esterification of waxy cassava starch on emulsifying properties in Pickering-type emulsions, LWT-foodSci. Technol. 91 (2018) 258–264, https://doi.org/10.1016/j.lwt.2018.01.057.

[5] R.V. Rios, R. Garzon, S.C.S. Lannes, C.M. Rosell, Use of succinyl chitosan as fat replacer on cake formulations, LWT-foodSci. Technol. 96 (2018) 260–265, https://doi.org/10.1016/j.lwt.2018.05.041.

[6] Z.Y. Yu, S.W. Jiang, Z. Zheng, X.M. Cao, Z.G. Hou, J.J. Xu, H.L. Wang, S.T. Jiang, L. J. Pan, Preparation and properties of OSA-modified taro starches and their application for stabilizing Pickering emulsions, Int. J. Biol. Macromol. 137 (2019) 277–285, https://doi.org/10.1016/j.ijbiomac.2019.06.230.

[7] T. Dapcevic-Hadnadev, M. Hadnadev, L. Dokic, V. Krstonosic, Small deformation rheological behaviour of wheat gluten - octenyl succinyl modified corn starches mixtures, J. Cereal Sci. 97 (2021), 103150, https://doi.org/10.1016/j.jcs.2020.103150.

[8] N.N. Shah, K.V. Umesh, R.S. Singhal, Hydrophobically modified pea proteins: synthesis, characterization and evaluation as emulsifiers in eggless cake, J. Food Eng. 255 (2019) 15–23, https://doi.org/10.1016/j.jfoodeng.2019.03.005.

[9] Y. Pan, Q.T. Xie, J. Zhu, X.M. Li, R. Meng, B. Zhang, H.Q. Chen, Z.Y. Jin, Study on the fabrication and in vitro digestion behavior of curcumin-loaded emulsions stabilized by succinylated whey protein hydrolysates, Food Chem. 287 (2019) 76–84, https://doi.org/10.1016/j.foodchem.2019.02.047.

[10] L.Y. Ren, J.Y. Liu, X.Q. Zhang, S.J. Zhao, Y. Lv, H.Y. Guo, Emulsion, gelation, physicochemical properties and microstructure of phosphorylated and succinylated egg yolk, LWT-Food Sci. Technol. 131 (2020), 109675, https://doi.org/10.1016/j.lwt.2020.109675.

[11] A. Agarwal, A.K. Pathera, R. Kaushik, N. Kumar, S.B. Dhull, S. Arora, P. Chawla, Succinylation of milk proteins: influence on micronutrient binding and functional indices, Trends Food Sci. Technol. 97 (2020) 254–264, https://doi.org/10.1016/j.tifs.2020.01.016.

[12] R.H. Wang, J.J. Wang, X.B. Guo, Y.F. Li, Y. Wu, H.Q. Liu, Y. Zhao, Physicochemical and functional properties of the Antarctic krill proteins modified by succinylation, LWT-Food Sci. Technol. 154 (2022), 112832, https://doi.org/10.1016/j.lwt.2021.112832.

[13] X. Xia, M. Ren, W.-S. He, C. Jia, X. Zhang, The preparation of phytosteryl succinyl sucrose esters and improvement of their water solubility and emulsifying properties, Food Chem. 373 (2022), 131501, https://doi.org/10.1016/j.foodchem.2021.131501.

[14] M. Falkeborg, Z. Guo, Dodecenyl succinylated alginate (DSA) as a novel dual-function emulsifier for improved fish oil-in-water emulsions, Food Hydrocoll. 46 (2015) 10–18, https://doi.org/10.1016/j.foodhyd.2014.12.011.

[15] M. Gharaghani, M. Mousavi, F. Khodaiyan, M.S. Yarmand, M. Omar-Aziz, S. S. Hosseini, Octenyl succinylation of kefiran: preparation, characterization and functional properties, Int. J. Biol. Macromol. 166 (2021) 1197–1209, https://doi.org/10.1016/j.ijbiomac.2020.11.002.

[16] W.Y. Li, A.X. Jin, C.F. Liu, R.C. Sun, A.P. Zhang, J.F. Kennedy, Homogeneous modification of cellulose with succinic anhydride in ionic liquid using 4-dimethylaminopyridine as a catalyst, Carbohydr. Polym. 78 (3) (2009) 389–395, https://doi.org/10.1016/j.carbpol.2009.04.028.

[17] G.T. Li, X. Xu, F. Zhu, Physicochemical properties of dodecenyl succinic anhydride (DDSA) modified quinoa starch, Food Chem. 300 (2019), 125201, https://doi.org/10.1016/j.foodchem.2019.125201.

[18] C.F. Liu, R.C. Sun, A.P. Zhang, J.L. Ren, X.A. Wang, M.H. Qin, Z.N. Chao, W. Luo, Homogeneous modification of sugarcane bagasse cellulose with succinic anhydride using an ionic liquid as reaction medium, Carbohydr. Res. 342 (7) (2007) 919–926, https://doi.org/10.1016/j.carres.2007.02.006.

[19] R.J. Moon, A. Martini, J. Nairn, J. Simonsen, J. Youngblood, Cellulose nanomaterials review: structure, properties and nanocomposites, Chem. Soc. Rev. 40 (7) (2011) 3941–3994, https://doi.org/10.1039/C0CS00108B.

[20] B. Baghaei, M. Skrifvars, All-cellulose composites: a review of recent studies on structure, properties and applications, Molecules 25 (12) (2020) 2836, https://doi.org/10.3390/molecules25122836.

[21] Z.Q. Li, Y. Zhang, S. Anankanbil, Z. Guo, Applications of nanocellulosic products in food: manufacturing processes, structural features and multifaceted functionalities, Trends Food Sci. Technol. 113 (2021) 277–300, https://doi.org/10.1016/j.tifs.2021.03.027.

[22] K. Karimi, M.J. Taherzadeh, A critical review of analytical methods in pretreatment of lignocelluloses: composition, imaging, and crystallinity, Bioresour. Technol. 200 (2016) 1008–1018, https://doi.org/10.1016/j.biortech.2015.11.022.

[23] Y. Jiang, G.B. Yu, Y. Zhou, Y.Y. Liu, Y.H. Feng, J.C. Li, Effects of sodium alginate on microstructural and properties of bacterial cellulose nanocrystal stabilized emulsions, Colloid Surf. A 607 (2020), 125474, https://doi.org/10.1016/j.colsurfa.2020.125474.

[24] Y. Hu, Z. Guo, B.M. Lue, X. Xu, Enzymatic synthesis of esculin ester in ionic liquids buffered with organic solvents, J. Agric. Food Chem. 57 (2009) 3845–3852, https://doi.org/10.1021/jf8037488.

[25] E. Krugly, I. Pauliukaityte, D. Ciuzas, M. Bulota, L. Peciulyte, D. Martuzevicius, Cellulose electrospinning from ionic liquids: the effects of ionic liquid removal on the fiber morphology, Carbohydr. Polym. 285 (2022), 119260, https://doi.org/10.1016/j.carbpol.2022.119260.

[26] P.S. Barber, C.S. Griggs, G. Gurau, Z. Liu, S. Li, Z.X. Li, X.M. Lu, S.J. Zhang, R. D. Rogers, Coagulation of chitin and cellulose from 1-Ethyl-3-methylimidazolium acetate ionic-liquid solutions using carbon dioxide, Angew. Chem. Int. Ed. 52 (47) (2013) 12350–12353, https://doi.org/10.1002/anie.201304604.

[27] C. Verma, A. Mishra, S. Chauhan, P. Verma, V. Srivastava, M.A. Quraishi, E. E. Ebenso, Dissolution of cellulose in ionic liquids and their mixed cosolvents: a review, Sustain. Chem. Pharm. 13 (2019), 100162, https://doi.org/10.1016/j.scp.2019.100162.

[28] D.M. Kalaskar, R.V. Ulijn, J.E. Gough, M.R. Alexander, D.J. Scurr, W.W. Sampson, S.J. Eichhorn, Characterisation of amino acid modified cellulose surfaces using ToF-SIMS and XPS, Cellulose 17 (4) (2010) 747–756, https://doi.org/10.1007/s10570-010-9413-y.

[29] S. Saska, R.M. Scarel-Caminaga, L.N. Teixeira, L.P. Franchi, R.A. dos Santos, A. Gaspar, P.T. de Oliveira, A. Rosa, C. Takahashi, Y. Messaddeq, S.J.L. Ribeiro, R. Marchetto, Characterization and in vitro evaluation of bacterial cellulose membranes functionalized with osteogenic growth peptide for bone tissue engineering, J. Mater. Sci.-Mater. M. 23 (9) (2012) 2253–2266, https://doi.org/10.1007/s10856-012-4676-5.

[30] L. Li, S. Zhao, J. Zhang, Z.X. Zhang, H.Q. Hu, Z.X. Xin, J.K. Kim, TEMPO-mediated oxidation of microcrystalline cellulose: influence of temperature and oxidation procedure on yields of water-soluble products and crystal structures of water-insoluble residues, Fiber Polym. 14 (3) (2013) 352–357, https://doi.org/10.1007/s12221-013-0352-8.

[31] A. Isogai, T. Hanninen, S. Fujisawa, T. Saito, Review: catalytic oxidation of cellulose with nitroxyl radicals under cob for aqueous conditions, Prog. Polym. Sci. 86 (2018) 122–148, https://doi.org/10.1016/j.progpolymsci.2018.07.007.

[32] M. Hirota, N. Tamura, T. Saito, A. Isogai, Oxidation of regenerated cellulose with NaClO2 catalyzed by TEMPO and NaClO under acid-neutral conditions, Carbohydr. Polym. 78 (2) (2009) 330–335, https://doi.org/10.1016/j.carbpol.2009.04.012.

[33] M. Hirota, N. Tamura, T. Saito, A. Isogai, Surface carboxylation of porous regenerated cellulose beads by 4-acetamide-TEMPO/NaClO/NaClO2 system, Cellulose 16 (5) (2009) 841–851. https://link.springer.com/article/10.1007/s10570-009-9296-y.

[34] M. Hirota, N. Tamura, T. Saito, A. Isogai, Water dispersion of cellulose II nanocrystals prepared by TEMPO-mediated oxidation of mercerized cellulose at pH 4.8, Cellulose 17 (2) (2010) 279–288.

[35] M. Hirota, N. Tamura, T. Saito, A. Isogai, Cellulose II nanoelements prepared from fully mercerized, partially mercerized and regenerated celluloses by 4-acetamido-TEMPO/NaClO/NaClO2 oxidation, Cellulose 19 (2) (2012) 435–442. https://link.springer.com/article/10.1007/s10570-009-9296-y.

[36] L. Segal, J.J. Creely, A. Martin Jr., C. Conrad, An empirical method for estimating the degree of crystallinity of native cellulose using the X-ray diffractometer, Text. Res. J. 29 (10) (1959) 786–794, https://doi.org/10.1177/004051755902901003.

[37] J. Revol, A. Dietrich, D. Goring, Effect of mercerization on the crystallite size and crystallinity index in cellulose from different sources, Can. J. Chem. 65 (8) (1987) 1724–1725. https://cdnsciencepub.com/doi/abs/10.1139/v87-288.

[38] K. Zhang, S. Fischer, A. Geissler, E. Brendler, Analysis of carboxylate groups in oxidized never-dried cellulose II catalyzed by TEMPO and 4-acetamide-TEMPO, Carbohydr. Polym. 87 (1) (2012) 894–900, https://doi.org/10.1016/j.carbpol.2011.08.090.

[39] S.R. Holmes-Farley, R.H. Reamey, T.J. McCarthy, J. Deutch, G.M. Whitesides, Acid-base behavior of carboxylic acid groups covalently attached at the surface of polyethylene: the usefulness of contact angle in following the ionization of surface functionality, Langmuir 1 (6) (1985) 725–740, https://doi.org/10.1021/la00066a016.

[40] Z. Li, S. Anankanbil, L. Li, J. Lyu, M. Nadzieja, Z. Guo, Alkylsuccinylated oxidized cellulose-based amphiphiles as a novel multi-purpose ingredient for stabilizing O/W emulsions, Food Hydrocoll. 134 (2023), 108014, https://doi.org/10.1016/j.foodhyd.2022.108014.

[41] G. Cheng, P. Varanasi, C.L. Li, H.B. Liu, Y.B. Menichenko, B.A. Simmons, M.S. Kent, S. Singh, Transition of cellulose crystalline structure and surface morphology of biomass as a function of ionic liquid pretreatment and its relation to enzymatic hydrolysis, Biomacromolecules 12 (4) (2011) 933–941, https://doi.org/10.1021/bm101240z.

[42] E. Kaffashsaie, H. Yousefi, T. Nishino, T. Matsumoto, M. Mashkour, M. Madhoushi, H. Kawaguchi, Direct conversion of raw wood to TEMPO-oxidized cellulose nanofibers, Carbohydr. Polym. 262 (2021), 117938, https://doi.org/10.1016/j.carbpol.2021.117938.

[43] M.I.H.A. Sohaimy, M.I.N.M. Isa, Natural inspired carboxymethyl cellulose (CMC) doped with ammonium carbonate (AC) as biopolymer electrolyte, Polymers 12 (11) (2020) 1–14, https://doi.org/10.3390/polym12112487, 2020.

[44] İ. Dinçer, A. Midilli, H. Kucuk, Progress in Sustainable Energy Technologies: Generating Renewable Energy, Springer, 2014.

[45] N. Lin, C. Bruzzese, A. Dufresne, TEMPO-oxidized nanocellulose participating as crosslinking aid for alginate-based sponges, ACS Appl. Mater. Inter. 4 (9) (2012) 4948–4959, https://doi.org/10.1021/am301325r.

[46] T. Inamochi, R. Funahashi, Y. Nakamura, T. Saito, A. Isogai, Effect of coexisting salt on TEMPO-mediated oxidation of wood cellulose for preparation of nanocellulose, Cellulose 24 (9) (2017) 4097–4101, https://doi.org/10.1007/s10570-017-1402-y.
[47] K. Chitbanyong, S. Pisutpiched, S. Khantayanuwong, G. Theeragool, B. Puangsin, TEMPO-oxidized cellulose nanofibril film from nano-structured bacterial cellulose derived from the recently developed thermotolerant komagataeibacter xylinus C30 and komagataeibacter oboediens R37–9 strains, Int. J. Biol. Macromol. 163 (2020) 1908–1914, https://doi.org/10.1016/j.ijbiomac.2020.09.124.
[48] I. Besbes, S. Alila, S. Boufi, Nanofibrillated cellulose from TEMPO-oxidized eucalyptus fibres: effect of the carboxyl content, Carbohydr. Polym. 84 (3) (2011) 975–983, https://doi.org/10.1016/j.carbpol.2010.12.052.
[49] Y. Zhou, X.C. Zhang, J.M. Zhang, Y.H. Cheng, J. Wu, J. Yu, J. Zhang, Molecular weight characterization of cellulose using ionic liquids, Polym. Testing 93 (2021), 106985, https://doi.org/10.1016/j.polymertesting.2020.106985.
[50] B. Puangsin, H. Soeta, T. Saito, A. Isogai, Characterization of cellulose nanofibrils prepared by direct TEMPO-mediated oxidation of hemp bast, Cellulose 24 (9) (2017) 3767–3775, https://doi.org/10.1007/s10570-017-1390-y.
[51] P. Huang, P. Zhang, L.J. Min, J.C. Tang, H.W. Sun, Synthesis of cellulose carbon aerogel via combined technology of wet ball-milling and TEMPO-mediated oxidation and its supersorption performance to ionic dyes, Bioresour. Technol. 315 (2020), 123815, https://doi.org/10.1016/j.biortech.2020.123815.
[52] F. He, J.H. Chen, Z.W. Gong, Q.Q. Xu, W. Yue, H.B. Xie, Dissolution pretreatment of cellulose by using levulinic acid-based protic ionic liquids towards enhanced enzymatic hydrolysis, Carbohydr. Polym. 269 (2021), 118271, https://doi.org/10.1016/j.carbpol.2021.118271.
[53] T. Isogai, T. Saito, A. Isogai, TEMPO electromediated oxidation of some polysaccharides including regenerated cellulose fiber, Biomacromolecules 11 (6) (2010) 1593–1599, https://doi.org/10.1021/bm1002575.
[54] K. Ahn, U. Hennniges, G. Banik, A. Potthast, Is cellulose degradation due to β-elimination processes a threat in mass deacidification of library books? Cellulose 19 (4) (2012) 1149–1159, https://doi.org/10.1007/s10570-012-9723-3.
[55] P. Gilna, L.R. Lynd, D. Mohnen, M.F. Davis, B.H. Davison, Progress in understanding and overcoming biomass recalcitrance: a BioEnergy science center (BESC) perspective, Biotechnol. Biofuels 10 (2017) 285, https://doi.org/10.1186/s13068-017-0971-1.
[56] B.P. Binks, Particles as surfactants - similarities and differences, Curr. Opin. Colloid. 7 (1–2) (2002) 21–41, https://doi.org/10.1016/S1359-0294(02)00008-0.
[57] G. Li, X. Xu, F. Zhu, Physicochemical properties of dodecenyl succinic anhydride (DDSA) modified quinoa starch, Food Chem. 300 (2019), 125201, https://doi.org/10.1016/j.foodchem.2019.125201.
[58] I. Kalashnikova, H. Bizot, B. Cathala, I. Capron, Modulation of cellulose nanocrystals amphiphilic properties to stabilize oil/water interface, Biomacromolecules 13 (1) (2012) 267–275, https://doi.org/10.1021/bm201599j.
[59] S. Tanpichai, S.K. Biswas, S. Witayakran, H. Yano, Optically transparent tough nanocomposites with a hierarchical structure of cellulose nanofiber networks prepared by the Pickering emulsion method, Compos. A: Appl. Sci. Manuf. 132 (2020), 105811, https://doi.org/10.1016/j.compositesa.2020.105811.
[60] E. Dickinson, Biopolymer-based particles as stabilizing agents for emulsions and foams, Food Hydrocoll. 68 (2017) 219–231, https://doi.org/10.1016/j.foodhyd.2016.06.024.